Regular Article

# The gyrokinetic water-bag modeling in toroidal geometry

R. Klein[1], E. Gravier[1,a], J.H. Chatenet[1], N. Besse[1], P. Bertrand[1], and X. Garbet[2]

[1] Institut Jean Lamour, UMR 7198 CNRS, Nancy Université, Bd des Aiguillettes, 54500 Vandoeuvre-lès-Nancy, France
[2] CEA, DSM, Institut de Recherche sur la Fusion Magnétique, Association Euratom-CEA, Cadarache,
13108 St-Paul-lez-Durance, France

**Abstract.** The present paper addresses the gyrokinetic water-bag model in toroidal geometry. The previous works were focused on the water-bag concept in magnetized cylindrical plasmas. Here we report on the possibility to improve the water-bag model by taking into account the curvature and gradient drifts. After a presentation of the model, a local linear analysis with some approximations is performed. Interchange and ion temperature gradient instabilities are examined with this new gyro-water-bag model in order to show its ability and its theoretical interest in describing kinetic instabilities in toroidal geometry.

## 1 Introduction

Micro-instabilities are now commonly held responsible for turbulence giving rise to anomalous radial energy transport in tokamak plasmas [1,2]. Such a turbulent transport governs the energy confinement time in controlled fusion devices. In this framework, the quest for performant discharges with good confinement properties relies crucially on the ability to accurately predict the level of turbulent transport.

Among these instabilities, ion temperature gradient (ITG), interchange instabilities, and trapped electron modes (TEM) may play an important role in explaining the anomalous heat and particle transport observed in tokamaks [2–4]. These instabilities are driven by ion and electron equilibrium gradients.

Numerical simulations can contribute to a better understanding of plasma instabilities. Fluid models are widely used. Solving three-dimensional 3D fluid equations is the most convenient way to compute the plasma response to the perturbed electromagnetic field when there is no wave-particle interaction and is all the more justified when Coulomb collisions are dominant. Moreover using fluid equations with an appropriate fluid closure [5,6] for nearly collisionless fusion plasmas in order to describe plasma turbulence is useful.

On the other hand, predicting turbulent transport in nearly collisionless fusion plasmas can be solved by using gyrokinetic equations [7] but is still a nontrivial task because of its demand of computer resources. This motivated us to revisit an alternative approach based on the water-bag (WB) representation of the distribution function [8]

which can be viewed as a useful tool to bring the bridge between fluid and kinetic models.

Introduced initially by DePackh [9], and Feix and co-workers [10–12], this model was extended into a double water-bag by Berk and Roberts [13], and Finzi [14], and generalized to the multiple water-bag [15–17]. It was shown to bring the bridge between fluid and kinetic descriptions of a collisionless and unmagnetized plasma, allowing one to keep the kinetic aspect of the problem with the same complexity as a multifluid model.

In recent work, we used the water bag model for magnetized plasmas in the framework of gyrokinetic modeling (gyro-water-bag, i.e. GWB model) in cylindrical geometry with a uniform and static magnetic field pointing in the axis direction. First, a linear study of the ITG instability in cylindrical geometry has been performed in the case of the drift-kinetic approximation without taking into account finite larmor radius (FLR) effects [8], polarization and gyroaveraging. It has been shown that the water-bag model converges rather rapidly towards that of the continuous distribution function (bag number $\geqslant 5$) when ITG instability linear growth rates are compared. Nonlinear numerical simulation has also been carried out in cylindrical geometry [18]. Next, a precise study of FLR effects on ITG instability has been performed [19]. Finally, a linear study of both collisional drift waves and ITG instabilities has been performed in the case of a linear magnetized plasma device [20]. This present work aims to report first linear results in toroidal geometry to show the capability of this GWB model in describing instabilities in toroidal geometry.

A gyro-water-bag model in toroidal geometry could be useful of course for non-linear simulations but also for linear studies. Indeed a comprehensive theoretical model for anomalous transport does not yet exist which can explain

a e-mail: etienne.gravier@ijl.nancy-universite.fr

the heat conductivity found in experiments. Most existing transport models are based on a mixing length rule based on quasi-linear theory [21]. In a number of cases the quasilinear approach exhibits a rather good agreement with experiments and recently nonlinear gyrokinetic simulations have been shown to scale almost as quasilinear predictions [22,23]. QuaLiKiz [21] is based on a fast linear gyrokinetic code, Kinezero [24]. In this code the fluctuating electrostatic potential frequency and wave-number spectra are chosen based on turbulence measurements and nonlinear simulations results. For Kinezero, the eigenfunction of the electrostatic potential is a trial function chosen to be a Gaussian with a width that has been benchmarked against nonlinear gyrokinetic codes. Such fluid or kinetic codes are useful for the integrated tokamak modeling. The purpose is to build a set of validated simulation tools, accessible and useful for ITER prediction and interpretation activity. In this frame the gyro-water-bag model could be an interesting linear tool, giving linear instability growth rates and exact eigenfunctions.

In this paper we address the problem of defining a gyro-water-bag model in toroidal axisymmetric geometry. In order to progress towards the description of tokamak plasmas, the present paper aims to demonstrate the relevance of the GWB model describing a strongly magnetized plasma in toroidal axisymmetric geometry. But here the eigenfunctions are not exactly solved but approximated in order to show in a first step the capability of the GWB model to describe instabilities and turbulence in toroidal geometry, namely by considering the toroidal curvature of the magnetic field lines and its consequences on the instabilities. Solving the exact problem is beyond the scope of this paper, and here the goal is not to know if the WB model could allow or not less costly numerical simulations. The main theoretical interest of the WB model in this toroidal geometry is to allow an easy local linear analysis without any constraint on the shape of the distribution function which can be very far from a Maxwellian, by taking into account energetic particles for instance.

The paper is organized as follows. In Section 2 the gyrokinetic model is described and the water-bag equations in toroidal geometry are introduced. The linear analysis of the new model is presented in Section 3. where the equilibrium and the first order dynamic are discussed. Next dispersion equation and results are given in Section 4. Interchange and ITG instabilities are investigated in toroidal axisymmetric geometry using this new gyro-water-bag model.

## 2 Gyrokinetic equations and water-bag modeling

### 2.1 The gyrokinetic model

Electromagnetic fluctuations in magnetized plasma fusion devices occur on time scales much longer than charged particle gyromotion period ($\omega/\Omega_c \ll 1$, where $\omega$ is the fluctuation frequency and $\Omega_c$ the cyclotron frequency).
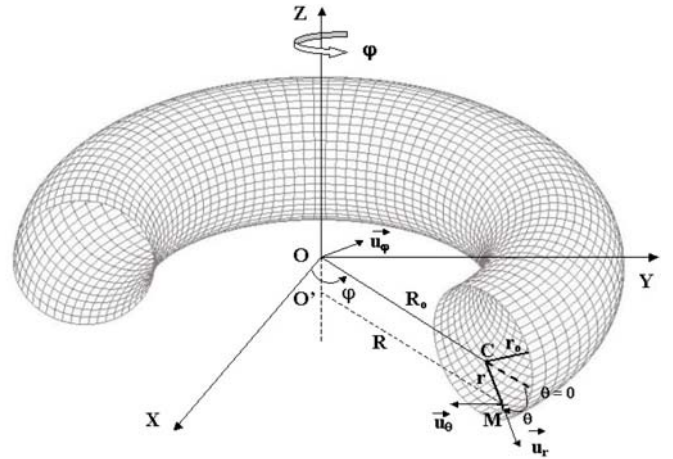


**Fig. 1.** Toroidal coordinates.

Moreover, the wavelength of these fluctuations is much smaller than the characteristic scale length of magnetic field $B/|\nabla B|$, density $n/|\nabla n|$, and temperature $T/|\nabla T|$ gradients. This gyrokinetic ordering [7] allows separation between fast gyromotion and slow dynamics in the perpendicular direction to the magnetic field. The phase space reduces to three dimensions in real space and two dimensions in velocity space. The particles are then described by a statistical distribution function $f(\mathbf{r}, v_\parallel, \mu, t)$ of their guiding-center (GC) position. The variable $v_\parallel$ is the velocity in the parallel direction to the magnetic field and $\mu = mv_\perp^2/2B$ is the first adiabatic invariant, which is linked to the perpendicular dynamic.

In this paper, a toroidal geometry is considered (see Fig. 1 for notations), and Coulomb collisions are neglected.

The magnetic field is of the form:

$$\mathbf{B}(r,\theta) = B_\theta \mathbf{u}_\theta + B_\varphi \mathbf{u}_\varphi \tag{1}$$

where $\varphi$ and $\theta$ are respectively the toroidal and poloidal coordinates. We assume $B_\theta$ smaller than $B_\varphi$ and the magnetic field lines to be curved with a radius of curvature $\mathbf{R}_c \sim \mathbf{R}$, with $\mathbf{R} = (R_0 + r\cos\theta)(\cos\theta\mathbf{u}_r - \sin\theta\mathbf{u}_\theta)$, $R_0$ being the major radius of the tore. The plasma parameters are supposed to be in the low-$\beta$ limit, i.e. the plasma pressure and volume currents are low. Therefore it is possible to write $\nabla B/B \simeq -\mathbf{R_c}/R_c^2$.

The gyrokinetic equations for ions then write [7,25,26]:

$$\partial_t f + \mathbf{v_D} \cdot \nabla f + \dot{v}_\parallel \partial_{v_\parallel} f = 0 \tag{2}$$

with
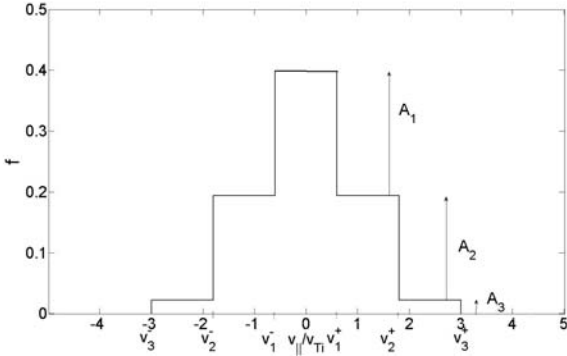
$$\mathbf{v}_D = v_\parallel \mathbf{b} + \mathbf{v}_{E\times B} + \mathbf{v}_c + \mathbf{v}_\nabla \tag{3}$$

$$\mathbf{v}_{E\times B} = -\frac{\nabla \mathcal{J}_\mu \phi \times \mathbf{b}}{B} \tag{4}$$

$$\mathbf{v}_c + \mathbf{v}_\nabla = \left(\frac{\mu}{q} + \frac{v_\parallel^2}{\Omega_c}\right)\frac{\mathbf{R} \times \mathbf{b}}{R^2} \tag{5}$$

$$\dot{v}_\parallel = -\left(\frac{q}{m_i}\nabla \mathcal{J}_\mu \phi + \frac{\mu}{m_i}\nabla B\right) \cdot \left(\mathbf{b} + \frac{v_\parallel}{\Omega_c}\frac{\mathbf{R} \times \mathbf{b}}{R^2}\right) \tag{6}$$

**Fig. 2.** Water-bag distribution function for $M = 3$ plotted against the parallel velocity.



**Fig. 3.** Bag contours in the phase space $x, v$ for a three-bag system. Between two contours, the distribution function $f$ remains equal to a constant $F_j$. The properties of the system are completely described by the knowledge of the contours.

where $f$ is the ion distribution function of the guiding centers for a given $\mu$, $\mathcal{J}_\mu$ is the gyroaverage operator [27]. The terms $q$ and $m_i$ are the ion charge and mass, $\mu$ is the first adiabatic invariant, and $\phi$ is the plasma potential. $\mathbf{b} = \mathbf{B}/B$ is the unit vector along the magnetic field.

The quasi-neutrality equation writes:

$$n_e = Z_i \left[ \mathcal{J}_\mu n_i + \nabla_\perp \cdot \left( \frac{n_{i_0}}{\Omega_c B} \nabla_\perp \phi \right) \right] \quad (7)$$

where the second term on the right-hand side corresponds to the polarization density. $n_i$ is the ion density, and $n_{i_0}$ is the ion density at the equilibrium. This equation is valid in the long wavelength approximation [28].
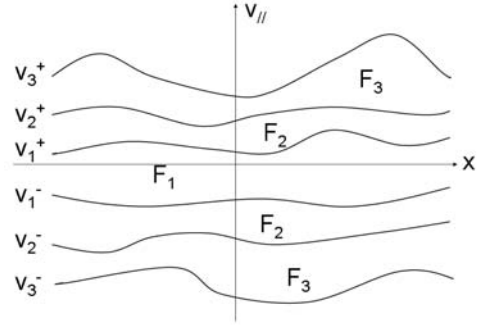
## 2.2 The water-bag model

The reader can refer to references [8,18–20] for a detailed presentation of the gyro-water-bag model, especially the method for choosing water-bag parameters. As seen above, gyrokinetic modeling makes full use of the $\mu$-invariance to eliminate perpendicular kinetic variables in the Vlasov equation. In the same way, the WB concept uses Liouville's invariance to reduce again the phase space dimension.

Using the same method that that of used in reference [8], an ion distribution function of the following form (Fig. 2) is chosen:

$$f_{MWB}(\mathbf{r}, v_\parallel, t) =$$
$$\sum_{j=1}^M A_j \left\{ H[v_\parallel - v_j^-(\mathbf{r}, t)] - H[v_\parallel - v_j^+(\mathbf{r}, t)] \right\} \quad (8)$$

where $M$ is the bag number, and $H$ is the Heaviside step-function.

The most interesting property of the WB distribution is the absolute time invariance of the different bag heights $A_j$. Consequently, the evolution of the system is entirely determined by the dynamical equations of the finite set of contours $v_j^+(\mathbf{r}, t)$ and $v_j^-(\mathbf{r}, t)$ (Fig. 3). Indeed, introducing this distribution function in the gyrokinetic

equations leads to the following set of equations, called contour equations [8]:

$$\partial_t v_j^\pm + \left[ \mathbf{v}_{E \times B} + \mathbf{v}_{(c + \nabla)_j} \right] \cdot \nabla_\perp v_j^\pm + v_j^\pm \nabla_\parallel v_j^\pm = \dot{v}_j^\pm \quad (9)$$

where

$$\mathbf{v}_{(c + \nabla)_j} = \left( \frac{\mu}{q} + \frac{v_j^{\pm 2}}{\Omega_c} \right) \frac{\mathbf{R} \times \mathbf{b}}{R^2}. \quad (10)$$

Thus the properties of the system are completely described by the knowledge of the contours $v_j^\pm$, which obey the motion equations. The right-hand side of the equation (9) is the same as the parallel acceleration in equation (6) except for the subscript $\parallel$ replaced by $j$. It can be seen like the acceleration of an ion placed in the contour $v_j^\pm$. These contours are coupled by the quasi-neutrality equation:

$$n_e = Z_i \left[ \mathcal{J}_\mu \sum_{j=1}^M A_j \left( v_j^+ - v_j^- \right) + \nabla_\perp \cdot \left( \frac{n_{i_0}}{\Omega_c B} \nabla_\perp \phi \right) \right]. \quad (11)$$

In these equations, $j$ is nothing but a label since no differential operation is carried on $v$. What we actually do is to bunch together particles within the same bag $j$, and let each bag evolves using contour equations (9). The kinetic equation is reduced into a set of hydrodynamic equations while keeping its kinetic character, the system behaves as $M$ fluids coupled together by the quasi-neutrality equation. There are as many hydrodynamic equations as bags, and no differential equation is carried out on the variable $v_\parallel$. To sum up, introducing both magnetic moment and Liouville invariance appears as an exact reduction in the phase space dimension elimination of $v_\perp$ and $v_\parallel$. Of course these eliminated velocities reappear as parameters in the various magnetic moments and bags. Since there is no mathematical lower bound on the bag number $M$, from a physical point of view, many interesting results can be obtained even with reasonably small numbers for $M$ [8]. Although this fact is commonly used in gyrokinetic theory, the further WB reduction should afford more analytical approaches, which are not restricted to Maxwellian distribution functions. The sampling $j$ allows to consider any arbitrary distribution along the parallel velocity $v_\parallel$.

# 3 Linear analysis of the ion population

The goal of this section is to perform a local linear analysis of the GWB equations in toroidal geometry. Water-bag equations can be solved by the procedure of linearization. As emphasized before the goal of this paper is not to solve exactly the equations but to show the capability of the water-bag model to describe ITG and Interchange instabilities in toroidal geometry. Consequently, the equations are simplified to point out this property. In this way the gyroaverage operator is taken to be equal to 1, and the polarization term in the quasi-neutrality equation is neglected (both terms are of second order in the gyrokinetic parameter $\omega/\Omega_c$).

We first separate the dependent variables into two parts: an equilibrium part and a perturbation part. The potential and the velocities write:

$$v_j^\pm = \pm a_j(r,\theta) + W_j^\pm(r,\theta)e^{i(n\varphi-\omega t)} \tag{12}$$

$$\phi_{tot} = \phi(r,\theta)e^{i(n\varphi-\omega t)} \tag{13}$$

where the Fourier toroidal mode $n$ is such that $n = Rk_\varphi$, $a_j$ is the velocity of the $j$th bag at the equilibrium, $W_j^\pm \exp[i(n\varphi-\omega t)]$ the velocity pertubation, and $\phi(r,\theta)\exp[i(n\varphi-\omega t)]$ the potential perturbation (there is no electric field at the equilibrium).

The GWB description is used for the ion population. This population is then described by equations (9) and (10).

## 3.1 Equilibrium

The equilibrium quantities express the state of the unperturbed plasma. By using equations (12) and (13) and retaining only terms at the zeroth order in perturbation the equation (9) writes:

$$\underbrace{\frac{a_j}{r}\frac{\partial a_j}{\partial\theta}}_{(1)} \mp \underbrace{\frac{b_\varphi}{b_\theta}\frac{\sin\theta}{R\Omega_c}\frac{\partial a_j}{\partial r}\left(a_j^2 + \frac{\mu B}{m_i}\right)}_{(2)}$$

$$\mp \underbrace{\frac{b_\varphi}{b_\theta}\frac{\cos\theta}{R\Omega_c}\frac{1}{r}\frac{\partial a_j}{\partial\theta}\left(a_j^2 + \frac{\mu B}{m_i}\right)}_{(3)} + \underbrace{\frac{\mu B}{m_i}\frac{\sin\theta}{R}}_{(4)} = 0 \tag{14}$$

where $b_\varphi = B_\varphi/B$ and $b_\theta = B_\theta/B$.

Assuming that the ion particle velocity in the parallel and perpendicular directions is close to $v_{Ti} = \sqrt{k_B T_{io}/m_i}$, the following ordering can be used:

– $\frac{b_\varphi}{b_\theta}\frac{r}{R} \simeq 1$
– $a_j \simeq v_{Ti}$
– $\mu = \frac{m_i v_\perp^2}{2B} \simeq qv_{Ti}^2/\Omega_c$ and $r_{Li} = v_{Ti}/\Omega_c$
– $\frac{1}{r}\frac{\partial a_j}{\partial\theta} \simeq \frac{v_{Ti}}{l_\theta}$ with $l_\theta \simeq r$
– $\frac{\partial a_j}{\partial r} \simeq \frac{v_{Ti}}{l_T}$ with $l_T \simeq r$

and considering the ratio of each term to other terms:

– $((2)+(3))/(1) \sim r_{Li}/R$
– $(4)/(1) \sim r/R$

it can be deduced that the terms (2) and (3) are smaller than (4) for a tokamak plasma, so terms (2) and (3) can be neglected in first approximation. Equation (14) then reduces to:

$$a_j\frac{\partial a_j}{\partial\theta} + \frac{\mu B}{m_i}\frac{r\sin\theta}{R} = 0. \tag{15}$$

This equation allows one to get the trapped/circulating particle behaviour and the trapping condition. By assuming $B/R \sim$ Const. when $\theta$ varies, $a_j$ writes:

$$a_j^2 = a_{j_0}^2 - \frac{2\mu B}{m_i}\frac{r}{R}(1-\cos\theta) \tag{16}$$

where $a_{j_0} = a_j(r,\theta=0)$. The condition for an ion to be trapped is $a_{j_0}^2 < \frac{2\mu B}{m_i}\frac{r}{R}$.

It can be noted that the approximate analytical solution by dropping term (2) and (3) of the zero-order waterbag equation (Eq. (14)) leading to equation (15) is very closed to the numerical solution of the complete zero-order nonlinear equation (14) – in term of zero-order bags – which can be seen as a first-order transport equation.

The evolution of $a_j$ is shown in Figure 4 for different values of $\theta$ and $\mu$. As a particle moves into a region of higher field-strength, e.g. towards $\theta = \pm\pi$, its velocity along the field decreases. And it is well known that in its back and forth motion from one turning point to the other, a trapped particle trajectory draws a banana-like shape when projected in the poloidal cross-section.
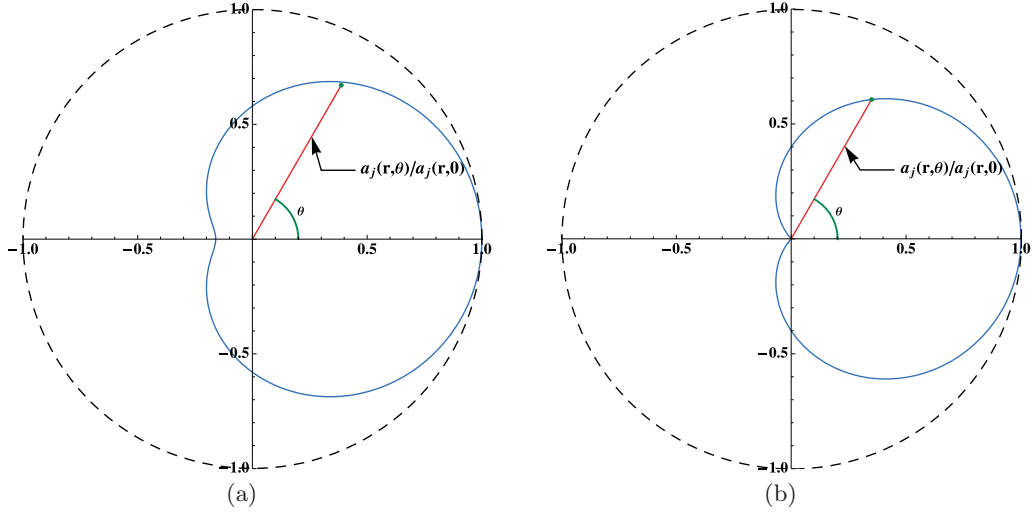
## 3.2 First order dynamic

Using equations (12) and (13) and neglecting the terms at second order with respect to the perturbation, the equation (9) writes:

$$\left[\omega + \delta_j - \beta_j - (e_j - d_j)\frac{1}{r}\frac{\partial}{\partial\theta} + f_j\frac{\partial}{\partial r}\right]W_j^+ =$$
$$\left[\chi + h_j - (\xi - k_j)\frac{1}{r}\frac{\partial}{\partial\theta} - r_j\frac{\partial}{\partial r}\right]\phi \tag{17}$$

and

$$\left[\omega - \delta_j - \beta_j - (e_j + d_j)\frac{1}{r}\frac{\partial}{\partial\theta} + f_j\frac{\partial}{\partial r}\right]W_j^- =$$
$$\left[\chi - h_j - (\xi + k_j)\frac{1}{r}\frac{\partial}{\partial\theta} + r_j\frac{\partial}{\partial r}\right]\phi \tag{18}$$

**Fig. 4.** (Color online) Equilibrium velocity $a_j$ plotted against $\theta$. (a) Circulating particule case: $a_j$ never cancels. (b) Trapped particle case: there is a critical value $\theta_L$ for which $a_j$ is zero. This value corresponds to the turning back point of particles.

where

$$\delta_j = i\frac{b_\theta}{r}\frac{\partial a_j}{\partial \theta} - a_j b_\varphi k_\varphi \tag{19}$$

$$\beta_j = 2i\frac{m_i}{qBR}a_j b_\varphi \left(\sin\theta\frac{\partial a_j}{\partial r} + \frac{\cos\theta}{r}\frac{\partial a_j}{\partial \theta}\right)$$
$$+ \frac{m_i}{qBR}\left(a_j^2 + \frac{\mu B}{m_i}\right)b_\theta \cos\theta k_\varphi \tag{20}$$

$$d_j = ia_j b_\theta \tag{21}$$

$$e_j = i\frac{m_i}{qBR}\left(a_j^2 + \frac{\mu B}{m_i}\right)b_\varphi \cos\theta \tag{22}$$

$$f_j = -i\frac{m_i}{qBR}\left(a_j^2 + \frac{\mu B}{m_i}\right)b_\varphi \sin\theta \tag{23}$$

$$\chi = k_\varphi b_\varphi \frac{q}{m_i} \tag{24}$$

$$h_j = \frac{k_\varphi}{B}b_\theta\frac{\partial a_j}{\partial r} + \frac{a_j}{RB}b_\theta \cos\theta k_\varphi \tag{25}$$

$$k_j = i\frac{b_\varphi}{B}\frac{\partial a_j}{\partial r} + i\frac{a_j}{RB}b_\varphi \cos\theta \tag{26}$$

$$\xi = i\frac{q}{m_i}b_\theta \tag{27}$$

$$r_j = i\frac{b_\varphi}{B}\left(\frac{1}{r}\frac{\partial a_j}{\partial \theta} - \frac{a_j}{R}\sin\theta\right). \tag{28}$$

Here a rough approximation is performed with the aim of going further. It consists in transforming the differential operator $\partial/\partial\theta$ by decomposing poloidal fluctuations into Fourier modes (this approximation is justified provided $R_C$ is large) and using a local approximation (only one poloidal mode is considered). The differential operator $\partial/\partial r$ is transformed by assuming an exponential radial profile of the amplitude of the fluctuations instead of solving the full differential equation:

$$W_j^\pm(r,\theta) = W_{j0}^\pm e^{g(r)}e^{im\theta} \tag{29}$$

$$\phi(r,\theta) = \phi_0 e^{g(r)}e^{im\theta}. \tag{30}$$

The ballooning representation makes use of the anistropy of instabilities ($k_\perp \gg k_\parallel$) to reduce the problem to one dimension only. At the lowest order of ballooning expansion the radial dependence can be neglected. In this paper the $\theta$-envelope is also neglected. This assumption can be seen as the ballooning calculation at the zeroth-order. Of course the local growth rate is an approximation of the global growth rate which is obtained by solving the global eigenvalues problem ($2D - r, \theta$) and particularly by solving the mode envelope. This task will be the matter for further studies.

Thanks to these assumptions ($W_j^+ - W_j^-$) can be factorized and the density perturbation $\delta n_{i_0}$ can be deduced from it because:

$$n_i = n_{i_0} + (\delta n_{i_0})e^{g(r)}e^{i(m\theta + n\varphi - \omega t)} \tag{31}$$

and:

$$n_i = \sum_{j=1}^{M} A_j(v_j^+ - v_j^-)$$
$$= \sum_{j=1}^{M} 2a_j A_j + \sum_{j=1}^{M} A_j(W_{j0}^+ - W_{j0}^-)e^{g(r)}e^{i(m\theta + n\varphi - \omega t)} \tag{32}$$

hence:

$$\delta n_{i_0} = \sum_{j=1}^{M} A_j(W_{j0}^+ - W_{j0}^-) \tag{33}$$

and the amplitude of the ion perturbation can be written as a function of the amplitude of the plasma potential:

$$\delta n_{i_0} = n_{i_0} \frac{\phi_0}{B} \sum_{j=1}^{M} \alpha_j \frac{N_1 c_j - N_{2j}(\omega - \omega_{1j})}{(\omega - \omega_{1j})^2 - c_j^2 a_j^2} \qquad (34)$$

where

$$\alpha_j = 2a_j A_j / n_{i_0} \qquad (35)$$

is the relative bag density and

$$N_1 = \Omega_c(k_\theta b_\theta + k_\varphi b_\varphi) \qquad (36)$$

$$N_{2j} = (k_\theta b_\varphi - k_\varphi b_\theta) \left( \frac{\cos\theta}{R} + \kappa_j \right)$$
$$+ i b_\varphi \frac{\partial g}{\partial r} \left( \frac{1}{r a_j} \frac{\partial a_j}{\partial \theta} - \frac{\sin\theta}{R} \right) \qquad (37)$$

$$c_j = k_\theta b_\theta + k_\varphi b_\varphi - i \frac{b_\theta}{r} \frac{1}{a_j} \frac{\partial a_j}{\partial \theta} \qquad (38)$$

$$\omega_{1j} = \frac{1}{R\Omega_c} \left[ (k_\varphi b_\theta - k_\theta b_\varphi) \left( a_j^2 + \frac{\mu B}{m_i} \right) \cos\theta \right]$$
$$+ i \frac{b_\varphi}{R\Omega_c} \left[ 2a_j^2 \left( \kappa_j \sin\theta + \frac{\cos\theta}{r} \frac{1}{a_j} \frac{\partial a_j}{\partial \theta} \right) \right.$$
$$\left. + \frac{\partial g}{\partial r} \left( a_j^2 + \frac{\mu B}{m_i} \right) \sin\theta \right]. \qquad (39)$$

# 4 Dispersion relation and results

Electrons are assumed to be very mobile and would be accelerated very quickly if there was a net force on them along the magnetic field lines. It applies to each magnetic field line separately, different lines may be charged to different potentials, so the electron response is taken adiabatic and satisfies the Boltzmann relation:
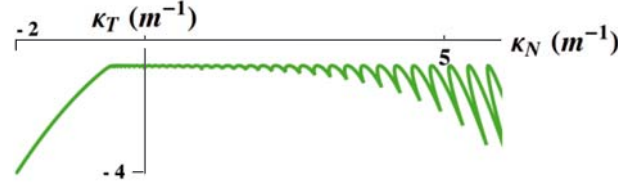
$$n_e = n_{eo} \exp \left[ \frac{e\phi_{tot}}{k_B T_e} \right]. \qquad (40)$$

Using the procedure of linearization for this equation and using the quasi-neutrality equation (11) in which the polarisation term is neglected, the dispersion relation then writes:

$$1 - \frac{k_B T_e}{eB} \sum_{j=1}^{M} \alpha_j \frac{N_1 c_j - N_{2j}(\omega - \omega_{1j})}{(\omega - \omega_{1j})^2 - c_j^2 a_j^2} = 0. \qquad (41)$$

It can be noted that the magnetic drift resonance is not depending on the water-bag distribution function, and is well captured by the dispersion relation through $w_{1j}$ which takes into account both curvature and magnetic gradient drifts.

As emphasized previously the goal of the paper is to show the ability of the GWB model to describe a large number of instabilities in toroidal geometry. Consequently we stress the effect due to the curvature and gradient



**Fig. 5.** (Color online) Linear stability diagram of the interchange instability in toroidal geometry in the $(\kappa_n, \kappa_T)$ plane. The following parameters are used: $M = 50$ in $\theta = 0$, and $T_i = 15$ keV, $T_e = 15$ keV, $k_\theta = 500$ m$^{-1}$, $R_0 = 6.2$ m, $r = 2 \times 10^{-1}$ m, $B = 5$ T, $\mu = 0$ J T$^{-1}$, $k_\varphi = 0$ m$^{-1}$.

drifts, making the following hypothesis to ensure our statement to be clear: from this point we specialize our general results to the particular case $b_\theta = 0$, $b_\varphi = 1$, the radial profile is assumed to be constant ($g(r) = 0$), $\partial a_j / \partial \theta = 0$ and $\mu = 0$ (ions are assumed to be highly circulating so that $\partial a_j / \partial \theta$ can be neglected). Indeed in this case a charged particle can not explore the poloidal cross section and consequently can not be trapped. According to this assumption and with the aim of studying the simplest case $\mu = 0$ is chosen for the following numerical examples.

## 4.1 Flute mode – interchange instability

In this section, the behavior of the pure electrostatic interchange instability in toroidal geometry [29–31] is investigated. With respect to the previous assumptions, a flute mode approximation is considered if $k_\varphi = 0$. Physical quantities do not depend on the toroidal coordinate $\varphi$.

The dispersion relation (41) then writes:

$$1 + \frac{k_B T_e}{eB} k_\theta \sum_{j=1}^{M} \alpha_j \frac{(\frac{\cos\theta}{R} + \kappa_j)(\omega - \omega_{1j})}{(\omega - \omega_{1j})^2} = 0 \qquad (42)$$

where
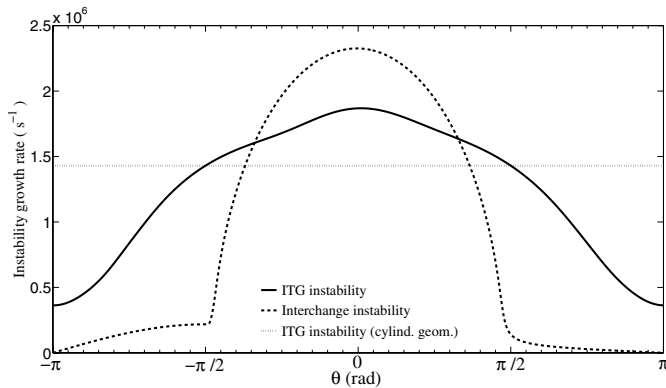
$$\omega_{1j} = \frac{a_j^2}{R\Omega_C}(-k_\theta \cos\theta + 2i\kappa_j \sin\theta). \qquad (43)$$

With respect to radial dependencies $\kappa_T = \partial_r \ln T_{i_0}$ and $\kappa_n = \partial_r \ln n_{i_0}$, the dispersion equation (42) may admit complex roots. The linear instability threshold is obtained by using a parametric approach relative to $\omega$, when Im($\omega$) becomes zero.

In Figure 5 the instability threshold is plotted for $M = 50$ in $\theta = 0$, and where $T_i = 15$ keV, $T_e = 15$ keV, $k_\theta = 500$ m$^{-1}$, $R_o = 6.2$ m, $r = 2 \times 10^{-1}$ m, $B = 5$ T, $\mu = 0$ J T$^{-1}$ (ions are assumed to be circulating) and $k_\varphi = 0$. The threshold is very closed to that of computed with a gyrokinetic model [30]. There are two distinct stable and unstable regions for negative temperature gradients. As expected, as the radial derivative of the equilibrium density becomes much negative the stability improves.

## 4.2 Ion temperature gradient (ITG) instability

We now consider the case of an ITG instability for which $k_\parallel = k_\varphi \neq 0$ ($b_\theta$ is chosen to be equal to zero with respect

**Fig. 6.** ITG ($k_\parallel \neq 0$) and interchange ($k_\parallel = 0$) instability growth rates plotted against $\theta$ in toroidal geometry, and for comparison ITG instability growth rate in cylindrical geometry ($R$ going to $\infty$ [8]).

to the previous assumption). The described modes corresponds to ITG instability.

The dispersion relation (41) then writes:

$$1 - \frac{k_B T_e}{eB} \sum_{j=1}^{M} \alpha_j \frac{k_\varphi^2 \Omega_C - k_\theta(\frac{\cos\theta}{R} + \kappa_j)(\omega - \omega_{1j})}{(\omega - \omega_{1j})^2 - k_\varphi^2 a_j^2} = 0 \tag{44}$$

where $\omega_{1j}$ is given by (43).

The ITG instability growth rate can be deduced from (44) and is plotted against $\theta$ (Fig. 6) for $\kappa_N = -1$ m$^{-1}$, $\kappa_T = -20$ m$^{-1}$, $M = 5$, $T_i = 15$ keV, $T_e = 15$ keV, $k_\theta = 500$ m$^{-1}$, $R_o = 6.2$ m, $r = 2 \times 10^{-1}$ m, $B = 5$ T, $\mu = 0$ J T$^{-1}$ and $k_\varphi = 5 \times 10^{-1}$ m$^{-1}$. For comparison the growth rate observed for ITG in cylindrical geometry, obtained by the GWB model in toroidal geometry when $R_C$ is going to infinity, is superposed. In these conditions the result is in total agreement with that of given by the GWB model in cylindrical geometry [8]. The instability growth rate in the case of interchange instability ($k_\varphi = 0$) in toroidal axisymmetric geometry is also superposed.

As one can see in Figure 6, as expected the disturbances are all the more unstable that the gradient of the plasma pressure and that of the magnetic field are of the same sign (low field side of the tokamak). This property is very well recovered in the case of the interchange instability, for which the growth rate is very close to zero at the strong field side of the torus. Nevertheless disturbances remain unstable at the strong field side, where the opposite sign of pressure and $B$ gradients strongly weakens the instability. This is where the Rayleigh-Taylor or interchange instability type is not superimposed on the cylindrical ITG instability.

Moreover the toroidal geometry has an important effect on instability growth rate: the growth rate is about 80% smaller in $\theta = \pi$ and 20% greater in $\theta = 0$ than that of given by the cylindrical model.

## 5 Conclusion

In this paper we have investigated the effects of the toroidal geometry (i.e curvature of the magnetic field lines) on the interchange and ITG instabilities using the new gyro-water-bag model. After some assumptions a linear eigenvalue equation has been derived and easily solved in the case of a local analysis. Using the water-bag model for the linear analysis allows interesting analytical studies and do not impose any constraint on the shape of the distribution function. The present results have to be extended in a forthcoming paper to include a complete analysis in poloidal direction and radial profiles not arbitrary estimated. Finite Larmor radius effects (polarization and gyroaveraging) and geodesic curvature also have to be included in the same way as in the cylindrical case to achieve a complete linear analysis. But these last aspects of the work are less difficult to handle than solving the complete $(r, \theta)$ differential equation without using the ballooning representation.

## References

1. A.M. Dimits, G. Bateman, M.A. Beer, B.I. Cohen, W. Dorland, G.W. Hammett, C. Kim, J.E. Kinsey, M. Kotschenreuther, A.H. Kritz, L.L. Lao, J. Mandrekas, W.M. Nevins, S.E. Parker, A.J. Redd, D.E. Shumaker, R. Sydora, J. Weiland, Phys. Plasmas **7**, 969 (2000)
2. X. Garbet, Plasma Phys. Control. Fusion **43**, A251 (2001)
3. L. Villard, S.J. Allfrey, A. Bottino, M. Brunetti, G.L. Falchetto, V. Grandgirard, R. Hatzky, J. Nührenberg, A. G. Peeters, O. Sauter, S. Sorge, J. Vaclavik, Nucl. Fusion **44**, 172 (2004)
4. T. Dannert, F. Jenko, Phys. Plasmas **12**, 072309 (2005)
5. J. Weiland, A. Zagorodny, V. Zasenko, AIP Conference Proceedings **1177**, 96 (2009)
6. A.M. Anile, G. Muscato, Phys. Rev. B **51**, 16728 (1995)
7. T.S. Hahm, Phys. Fluids **31**, 2670 (1988)
8. P. Morel, E. Gravier, N. Besse, R. Klein, A. Ghizzo, P. Bertrand, X. Garbet, P. Ghendrih, V. Grandgirard, Y. Sarazin, Phys. Plasmas **14**, 112109 (2007)
9. D.C. DePackh, J. Electron. Control **13**, 417 (1962)
10. M.R. Feix, F. Hohl, L.D. Staton, *Nonlinear effects in Plasmas* (Kalmann and Feix Editors, Gordon and Breach, 1969), pp. 3–21
11. P. Bertrand, M.R. Feix, Phys. Lett. A **28**, 68 (1968)
12. P. Bertrand, M.R. Feix, Phys. Lett. A **29**, 489 (1969)

13. H.L. Berk, K.V. Roberts, The water bag model, in *Methods in Computational Physics* (Academic Press, 1970), Vol. 9
14. U. Finzi, Plasma Phys. **14**, 327 (1972)
15. M. Navet, P. Bertrand, Phys. Lett. A **34**, 117 (1971)
16. P. Bertrand, J.P. Doremus, G. Baumann, M.R. Feix, Phys. Fluids **15**, 1275 (1972)
17. P. Bertrand, M. Gros, G. Baumann, Phys. Fluids **19**, 1183 (1976)
18. N. Besse, P. Bertrand, P. Morel, E. Gravier, Phys. Rev. E **77**, 056410 (2008)
19. R. Klein, E. Gravier, P. Morel, N. Besse, P. Bertrand, Phys. Plasmas **16**, 082106 (2009)
20. E. Gravier, R. Klein, P. Morel, N. Besse, P. Bertrand, Phys. Plasmas **15**, 122103 (2008)
21. C. Bourdelle, X. Garbet, F. Imbeaux, A. Casati, N. Dubuit, R. Guirlet, T. Parisot, Phys. Plasmas **14**, 112501 (2007)
22. F. Jenko, T. Dannert, C. Angioni, Plasma Phys. Control. Fusion **47**, B195 (2005)
23. G.M. Staebler, J.E. Kinsey, R.E. Waltz, Phys. Plasmas **12**, 102508 (2005)
24. C. Bourdelle, X. Garbet, G.T. Hoang, J. Ongena, R.V. Budny, Nucl. Fusion **42**, 892 (2002)
25. A.J. Brizard, T.S. Hahm, Rev. Mod. Phys. **79**, 421 (2007)
26. X. Garbet, Y. Sarazin, V. Grandgirard, G. Dif-Pradalier, G. Darmet, Ph. Gendrih, P. Angelino, P. Bertrand, N. Besse, E. Gravier, P. Morel, E. Sonnendrucker, N. Crouseilles, J.M. Dischler, G. Latu, E. Violard, M. Brunetti, S. Brunner, X. Lapillone, T. Tran, L. Villard, M. Boulet, Nucl. Fusion **47**, 1206 (2007)
27. F.R. Hansen, G. Knorr, J.P. Lynov, H.L. Pesceli, J.J. Rasmussen, Plasma Phys. Control. Fusion **31**, 173 (1989)
28. W.W. Lee, R.A. Kolesnikov, Phys. Plasmas **16**, 044506 (2009)
29. H. Wernefalk, J. Weiland, Phys. Scr. **51**, 789 (1995)
30. Y. Sarazin, V. Grandgirard, E. Fleurence, X. Garbet, P. Ghendrih, P. Bertrand, G. Depret, Plasma Phys. Control. Fusion **47**, 1817 (2005)
31. P. Ricci, B.N. Rogers, Phys. Rev. Lett. **104**, 145001 (2010)
32. J. Weiland, *Collective modes in inhomogeneous plasma* (Institute of Physics Publishing, 2000), pp. 61−63